Selective Inhibition of Human Brain Tumor Cells through Multifunctional Quantum-Dot-Based siRNA Delivery**

*Jongjin Jung, Aniruddh Solanki, Kevin A. Memoli, Ken-ichiro Kamei, Hiyun Kim, Michael A. Drahl, Lawrence J. Williams, Hsian-Rong Tseng, and KiBum Lee**

One of the most promising new chemotherapeutic strategies is the RNA interference (RNAi)-based approach, wherein small double-stranded RNA molecules can sequence-specifically inhibit the expression of targeted oncogenes.[1] In principle, this method has high specificity and broad applicability for chemotherapy. For example, the strategy of small interfering RNA (siRNA) enables manipulation of key oncogenes that modulate signaling pathways and thereby regulate the behavior of malignant tumor cells. To harness the full potential of this approach, the prime requirements are to deliver the siRNA molecules with high selectivity and efficiency into tumor cells and to monitor both siRNA delivery and the resulting knockdown effects at the single-cell level. Although several approaches such as polymer- and nanomaterial-based methods[2] have been attempted, limited success has been achieved for delivering siRNA into the target tumor cells. Moreover, these types of approaches mainly focus on the enhancement of transfection efficiency, knockdown of non-oncogenes (e.g. the gene coding for green fluorescent protein (GFP)), and the use of different nanomaterials such as quantum dots (QDs), iron oxide nanoparticles, and gold nanoparticles.[3,4] Therefore, to narrow the gap between current nanomaterial-based siRNA delivery and chemotherapies, there is a clear need to develop methods for target-oriented delivery of siRNA,[5] for further monitoring the effects of siRNA-mediated target-gene silencing by means of molecular imaging probes,[4] and for investigating the corresponding up/down-regulation of signaling cascades.[6] Perhaps most importantly, to begin the development of the necessary treatment modalities, the strategies for nanomaterial-based siRNA delivery must be demonstrated on oncogenes involved in cancer pathogenesis.

Herein, we describe the synthesis and target-specific delivery of multifunctional siRNA–QD constructs for selectively inhibiting the expression of epidermal growth factor receptor variant III (EGFRvIII) in target human U87 glioblastoma cells, and subsequently monitoring the resulting down-regulated signaling pathway with high efficiency.[7]

Glioblastoma multiforme (GBM) is the most malignant, invasive, and difficult-to-treat primary brain tumor. Successful treatment of GBM is rare with a mean survival of only 10–12 months.[8] EGFRvIII, the key growth factor receptor triggering cancer cell proliferation in many cancer diseases such as brain tumors and breast cancer, is a constitutively active mutant of EGFR which is expressed in only human GBM and several other malignant cancers, but not in normal healthy cells (Figure 1 A).[9] We targeted EGFRvIII, since it is known that knockdown of this gene is one of the most effective ways to down-regulate the PI3K/Akt signaling pathway, a key signal cascade for cancer cell proliferation and apoptosis.[6,10] Hence by targeting EGFRvIII, our siRNA delivery strategy based on multifunctional nanoparticles
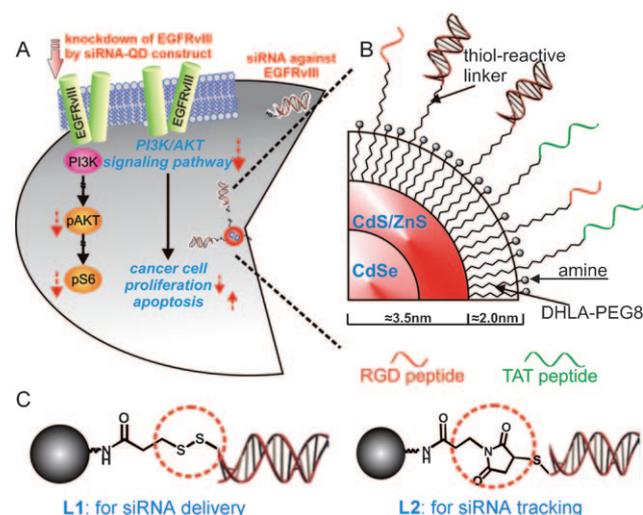
[*] J. Jung, A. Solanki, K. A. Memoli, H. Kim, M. A. Drahl, Prof. L. J. Williams, Prof. K.-B. Lee
Department of Chemistry and Chemical Biology, Rutgers University
Piscataway, NJ 08854 (USA)
Fax: (+1) 732-445-5312
E-mail: kblee@rutgers.edu
Homepage: http://rutchem.rutgers.edu/~kbleeweb/
Dr. K. Kamei, Prof. H.-R. Tseng
Department of Molecular and Medical Pharmacology
University of California, Los Angeles
Los Angeles, CA 90095 (USA)

Figure 1. A) Quantum dots as a multifunctional nanoplatform to deliver siRNA and to elucidate the EGFRvIII-knockdown effect of PI3K signaling pathway in U87-EGFRvIII B) Detailed structural information of multifunctional siRNA–QDs. C) Two different strategies for the siRNA–QD conjugate. **L1** shows the linker for attaching siRNA to QDs through a disulfide linkage which is easily reduced within the cells to release the siRNA. **L2** shows the linker for covalently conjugating siRNA to QDs which enables the tracking of siRNA–QDs within the cells.

Angew. Chem. Int. Ed. **2010**, *49*, 103–107

© 2010 Wiley-VCH Verlag GmbH & Co. KGaA, Weinheim

103

could potentially minimize the side effects caused by conventional chemotherapies, specifically immune suppression, while significantly improving the efficacy of chemotherapy against GBM.

We prepared two types of siRNA–QD conjugates, one for siRNA delivery and the other for siRNA tracking (Figure 1 B,C). Core–shell CdSe/CdS/ZnS QDs with a diameter of 7 nm were synthesized[11] and coated with either trioctylphosphine oxide (TOPO) or hexadecylamine (HDA). In order to make the QD constructs water-soluble and suitable for conjugating with siRNA, we displaced these hydrophobic ligands with a dihydrolipoic acid (DHLA) derivatized with an amine-terminated poly(ethylene glycol) (PEG) spacer. The expectation was that the dithiol moiety would provide strong coordination to the QD surface and increase stability in aqueous media, the PEG spacer would increase water solubility and reduce nonspecific binding, and the amine group would enable conjugation to the siRNA element.[12] Two bifunctional linkers were synthesized and evaluated for siRNA conjugation. The linker shown in **L1**, PTPPf [3-(2-pyridyl)-dithiopropionic acid pentafluorophenyl ester], was designed to release siRNA upon entering the cell by cleavage of the disulfide linkage, through enzymatic reduction or ligand exchange (e.g. glutathione).[13] The linker in **L2**, MPPF (3-maleimidopropionic acid pentafluorophenyl ester), was designed to be more robust, thereby enabling evaluation of cellular uptake and localization of the siRNA construct within the cellular compartments.[14] Details of the synthesis, characterization and conjugation protocols are given in the Supporting Information.

The final design component was functionalizing the construct for tumor-cell-selective transfection. For this purpose two functional peptides, thiol-modified RGD peptide and thiol-modified HIV-Tat derived peptide, were attached to the siRNA–QDs by the conjugation methods described above. Brain tumor cells (U87 and U87-EGFRvIII) overexpress the integrin receptor protein $\alpha_v\beta_3$, which strongly binds to the RGD binding domain.[15] RGD-functionalized siRNA–QDs selectively accumulate in brain tumor cells in vitro, and can be tracked by fluorescence microscopy.[16] In addition, the HIV-Tat peptide enables efficient transfection of siRNA–QDs in cells when it is directly attached to the QD surface.[17] The density of siRNA on the QDs and the ratio between siRNA strands and peptides were optimized for gene knockdown. It was found that the density of 10 siRNAs per nanoparticle and the ratio of 1:10 (siRNA for each peptide), which was in close agreement with literature values,[4] was optimal for knocking down the target genes (EGFP and EGFRvIII) overexpressed in our U87 cell lines.

To optimize gene silencing with our siRNA–QD constructs and to assess the transfection efficiency and RNA interference (RNAi) activity, we examined the suppression of EGFP expressed in U87 cell lines that were genetically modified to express EGFP. The cytotoxicity of the constructs was determined by serial dilution studies. The range of concentration causing minimal or negligible cytotoxicity was identified, and subsequent experiments employed the concentrations within this range (see Figure S1 in the Supporting Information).[18] Importantly, the EGFP cell line has been widely used to investigate siRNA-based silencing of EGFP, since the suppression of EGFP expression does not compromise cell viability. The transfection efficiency of three different kinds of constructs were evaluated; constructs modified with the RGD peptide only, those modified with the HIV-Tat peptide only, and those with both HIV-Tat and RGD peptide. Although the siRNA–QDs modified with only RGD showed considerable selective internalization within U87-EGFP cells, siRNA–QDs modified with a combination of RGD and HIV-Tat peptides (the ratio of siRNA/RGD/HIV-Tat being 1:10:10 per QD) showed maximum internalization within U87-EGFP cells, in close agreement with previous studies.[4] This optimal condition was used for subsequent siRNA–QD experiments.

The U87-EGFP cell line was then treated with siRNA–QDs (siRNA/QDs = 0.12 μM:0.011 μM), modified with HIV-Tat [≈1.2 μM] and RGD [≈1.2 μM], and simultaneously imaged using fluorescence microscopy (Figure 2). Cationic lipids (X-tremeGENE, Roche) were used to further enhance cellular uptake and prevent degradation of the siRNA within the endosomal compartment of the cells. The siRNA–QDs showed significant internalization into the cells. Knockdown of the EGFP signal was observed after 48–72 h (Figure 2 B). Fluorescence intensity was influenced by other factors such as exposure time, media conditions, and cell shrinkage. To minimize the influence from these external factors, the
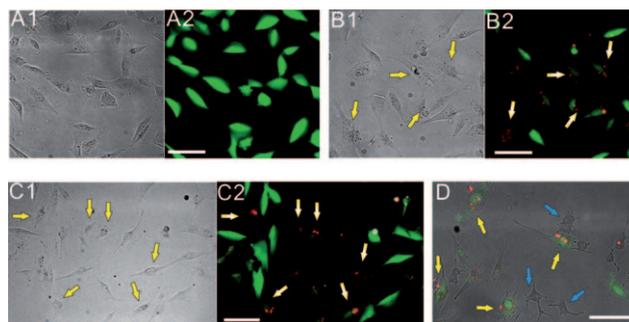

Figure 2. Knockdown of EGFP in U87 cells using siRNA–QDs modified with RGD and HIV-Tat peptides. (Note that yellow arrows mark U87-EGFP cells transfected with the siRNA–QDs and the blue arrows indicate PC-12 cells.) A) Control U87-EGFP cells without siRNA–QDs; phase-contrast image (A1) and the corresponding fluorescence image (A2). B) EGFP knockdown using multifunctional siRNA–QDs; B1) Phase-contrast image shows that the morphology of U87-EGFP cells has not changed relative to the control cells in (A). B2) Fluorescence image clearly shows the knockdown of EGFP in cells (marked by yellow arrows) which have internalized the siRNA–QDs (red) after 48 h. C) U87-EGFP control cells (without siRNA–QDs) and U87-EGFP cells transfected with siRNA–QDs were cocultured so as to investigate them under the same conditions; C1) Phase-contrast image clearly shows no difference in the morphology of the U87-EGFP control cells and the siRNA–QDs transfected cells. C2) Fluorescence image clearly shows the decrease in the EGFP signal in the U87-EGFP cells transfected with siRNA–QDs as compared to the surrounding U87-EGFP control cells. D) Phase-contrast image showing the target-oriented delivery of siRNA–QDs in cocultures of the malignant U87-EGFP cells, overexpressing the $\alpha_v\beta_3$ integrin receptors, and the less tumorigenic PC-12 cells (blue arrows) incubated with the siRNA–QDs. It can be clearly seen that most of the siRNA–QDs, owing to the presence of RGD and HIV-Tat peptides, were taken up by the U87-EGFP cells and not by the PC-12 cells. Scale bars: 100 μm.

control U87-EGFP cells (without siRNA) were trypsinized and co-cultured with U87-EGFP cells transfected with siRNA–QDs in the same well. The U87 cells containing siRNA–QDs were easily distinguishable from the control cells owing to the bright fluorescence of the QDs (Figure 2 C2). Cells with internalized siRNA–QDs showed considerable knockdown of the EGFP protein relative to the surrounding control U87-EGFP cells (Figure 2 C).

To further demonstrate the target-specific delivery of the siRNA–QDs, we incubated the siRNA–QDs modified with Tat and RGD against EGFP in co-cultures of the U87-EGFP cell line with other less-tumorigenic cell lines, such as PC-12 and SK-N-BE(2)C (see Figure S2 in the Supporting Information), which have a considerably small number of integrin receptors.[19] The presence of RGD tripeptide molecules on the surface of the siRNA–QDs led to specific binding with integrin receptors overexpressed in the U87 cells, resulting in higher cellular uptake by the malignant U87 cells than by the less tumorigenic PC-12 cells as seen by the selective accumulation of the QDs within the U87-EGFP cells (Figure 2 D). These results confirmed our hypothesis that the target-specific delivery of the siRNA–QDs into brain cancer cells can be significantly enhanced by functionalizing the QDs with targeting moieties like RGD tripeptide.

The intracellular delivery of the siRNA–QDs within the U87-EGFP cells was also confirmed by transmission electron microscopy (TEM), which clearly shows the presence of QDs in the cytoplasm of the cells (Figure 3 A). The knockdown efficiency of the siRNA–QDs was similar to or slightly better than that of the positive control consisting of U87-EGFP cells transfected with only siRNA using X-tremeGENE (see Figure S3 in the Supporting Information). This high transfection efficiency appears to result from synergistic effects of the two transfection peptides. Decrease in fluorescence intensities (EGFP signal, green fluorescence) within cells treated with the above-mentioned systems were then compared with the intensity of U87-EGFP without siRNA. As shown in (Figure 3 B), the decrease in fluorescence intensity of U87-EGFP incubated with siRNA–QDs and siRNA alone was comparable, but drastically lower than that observed for the control without siRNA. Cells containing siRNA–QDs show a weaker green fluorescence (EGFP signal) than the control. This data strongly suggests that siRNA–QDs can be used simultaneously as delivery and imaging probes.

Having demonstrated the selective manipulation of the U87-EGFP cell line, we then focused on the knockdown of EGFRvIII with our siRNA–QD constructs. U87-EGFRvIII cells were genetically modified to overexpress EGFRvIII, a mutant-type epidermal growth factor receptor (EGFR) only expressed within cancer cells.[20] This cell type was incubated with our siRNA–QDs modified with Tat and RGD peptides and armed with EGFRvIII-targeting siRNA. The cells were simultaneously imaged for the internalization of siRNA–QDs using fluorescence microscopy. Significant cell death was observed in the wells loaded with siRNA–QDs against EGFRvIII after 48 h (Figure 4 A). Quantitative analysis revealed that the number of viable U87-EGFRvIII cells, as observed by fluorescence microscopy, decreased with increasing incubation time. Relative to the control (U87-EGFRvIII
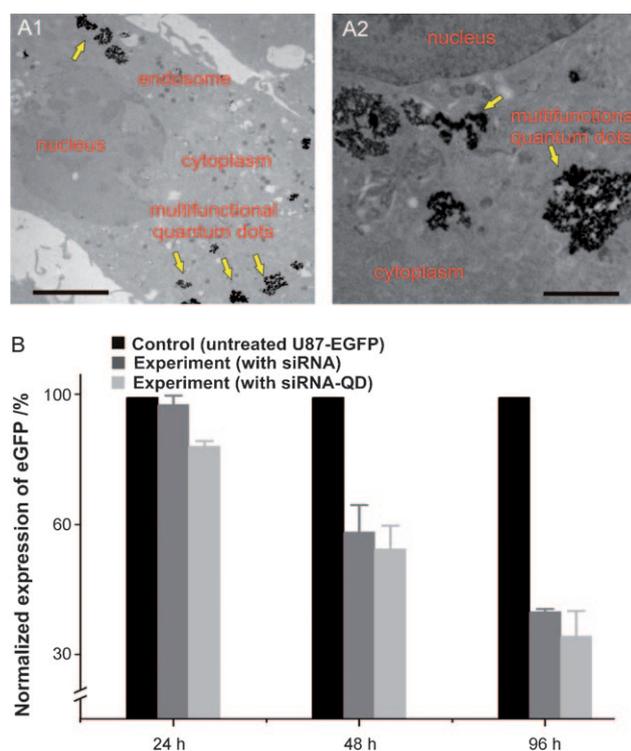

Figure 3. Knockdown efficiency of EGFP within U87-EGFP cells and internalization of multifunctional siRNA–QDs. A) TEM analysis of the internalization of the multifunctional siRNA–QDs into the U87-EGFP cells; A1) Presence of multifunctional siRNA–QDs (yellow arrows) within the cytoplasm and the endosome (scale bar: 5 μm). A2) Enlarged image showing individual siRNA–QDs within the cytoplasm (scale bar: 2.5 μm). B) The bar graph represents the knockdown of EGFP over 24 h, 48 h, and 96 h in U87-EGFP cells treated with siRNA [0.12 μM] only (dark gray), and siRNA–QD [siRNA:QD = 0.12 μM:0.011 μM] (light gray). The EGFP knockdown data was normalized with the expression levels of EGFP in the control U87-EGFP cells (black).

without siRNA–QDs), there was a significant decrease in the number of viable cells, thus demonstrating the effectiveness of our nanoparticle-based siRNA delivery to knockdown the oncogene. The result was confirmed using the MTT assay which showed a decrease in the number of viable cells in the well incubated with siRNA–QDs against EGFRvIII (Figure 4 B). This assay further confirmed that the QDs themselves were noncytotoxic when used alone as they did not result in any appreciable cell death (see Figure S1 in the Supporting Information). The knockdown of EGFRvIII and the inhibition of the downstream proteins in the PI3K signaling pathway were confirmed using Western immunoblotting. The results (Figure 4 C) confirm a considerable decrease in the expression of EGFRvIII, and down-regulation of phospho-Akt and phospho-S6 relative to the control. Thus, these results demonstrate the specificity of the siRNA against EGFRvIII, the inherent noncytotoxicity of the QDs, and the facile evaluation and manipulation of cancer cell proliferation with multifunctional QD constructs.

In summary, we have demonstrated an application of multifunctional siRNA–QDs focusing on targeted delivery, high transfection efficiency, and multimodal imaging/track-
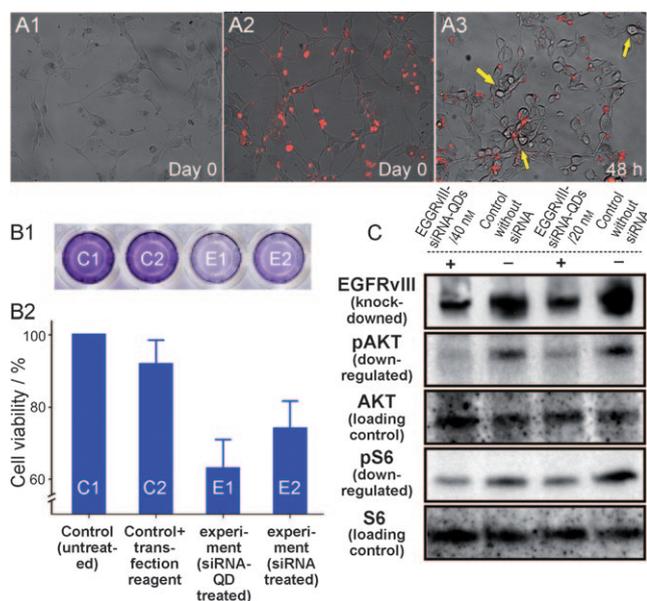
Figure 4. Knockdown of EGFRvIII in U87-EGFRvIII using multifunctional siRNA–QDs. A) Phase-contrast images showing the internalization of siRNA–QDs into the U87-EGFRvIII cells. A1) Morphology of U87-EGFRvIII cells before incubation with siRNA–QDs on Day 0. A2) U87-EGFRvIII cells after incubation with siRNA–QDs (red) on Day 0. A3) Morphology of U87-EGFRvIII cells 48 h after incubation with siRNA–QDs. Note that effect of the EGFRvIII knockdown by the siRNA–QDs can be clearly seen as the cells have clearly shrunk (yellow arrows) and appear to have collapsed (cf. Day 0), marking the onset of apoptosis; scale bar: 100 μm. B) Cell viability assay using MTT assay. B1) Optical image of cell viability (MTT) assay in a well plate. Dark blue color indicates a high number of viable cells and pale blue indicates a low population of viable cells. B2) MTT-assayed wells were quantified with UV absorbance and the data was converted to cell viability data. Untreated control C1 and C2 represent control cell population and viable cell population, respectively, in the presence of a cationic lipid based transfection reagent. siRNA–QD-transfected cells in experiment E1 and siRNA treated cells in E2 show low numbers of the viable cells due to knockdown of EGFRvIII gene. C) Western immunoblotting shows the silencing effect of the EGFRvIII gene. Protein expression level of EGFRvIII is dramatically decreased, and phosphorylation levels of key proteins in PI3K signaling pathway are reduced significantly. The upstream protein (AKT) and the downstream protein (S6), which play an important role in cell proliferation, are selected to investigate the gene-knockdown effect on the PI3K signaling pathway.

ing. Our siRNA–QDs could be used for the development of novel chemotherapies and diagnostics relevant to brain cancer research. These novel methods and applications complement recent advances in nanomaterial-based siRNA delivery, nanomaterial-based molecular imaging, and siRNA-based chemotherapeutic strategies reported recently. While the ability to functionalize as well as control the surface of quantum dots with specific linkers and multifunctional molecules (siRNA and peptides) is critical for nanoparticle-based drug delivery, this method could also provide highly useful information regarding biological surface chemistry of nanomaterials. In addition, the application of multifunctional siRNA–QDs to modulate the key cancer signaling pathways is important not only for selective chemotherapeutic strat-

egies but also for dissecting signaling cascades triggered by inhibiting specific proteins. Collectively, our strategy for siRNA delivery based on multifunctional QDs has significant potential for simultaneous prognosis, diagnosis, and therapy.

[1] a) Z. Medarova, W. Pham, C. Farrar, V. Petkova, A. Moore, *Nat. Med.* **2007**, *13*, 372–377; b) D. M. Dykxhoorn, D. Palliser, J. Lieberman, *Gene Ther.* **2006**, *13*, 541–552.

[2] a) L. Wasungu, D. Hoekstra, *J. Controlled Release* **2006**, *116*, 255–264; b) J. H. Jeong, H. Mok, Y. K. Oh, T. G. Park, *Bioconjugate Chem.* **2009**, *20*, 5–14; c) M. L. Patil, M. Zhang, S. Betigeri, O. Taratula, H. He, T. Minko, *Bioconjugate Chem.* **2008**, *19*, 1396–1403; d) A. Zintchenko, A. Philipp, A. Dehshahri, E. Wagner, *Bioconjugate Chem.* **2008**, *19*, 1448–1455.

[3] a) J. H. Lee, K. Lee, S. H. Moon, Y. Lee, T. G. Park, J. Cheon, *Angew. Chem.* **2009**, *121*, 4238–4243; *Angew. Chem. Int. Ed.* **2009**, *48*, 4174–4179; b) L. F. Qi, X. H. Gao, *Acs Nano* **2008**, *2*, 1403–1410; c) J. S. Lee, J. J. Green, K. T. Love, J. Sunshine, R. Langer, D. G. Anderson, *Nano Lett.* **2009**, *9*, 2402–2406; d) M. V. Yezhelyev, L. F. Qi, R. M. O'Regan, S. Nie, X. H. Gao, *J. Am. Chem. Soc.* **2008**, *130*, 9006–9012; e) D. A. Giljohann, D. S. Seferos, A. E. Prigodich, P. C. Patel, C. A. Mirkin, *J. Am. Chem. Soc.* **2009**, *131*, 2072.

[4] A. M. Derfus, A. A. Chen, D. H. Min, E. Ruoslahti, S. N. Bhatia, *Bioconjugate Chem.* **2007**, *18*, 1391–1396.

[5] a) R. Kikkeri, B. Lepenies, A. Adibekian, P. Laurino, P. H. Seeberger, *J. Am. Chem. Soc.* **2009**, *131*, 2110; b) A. A. Bhirde, V. Patel, J. Gavard, G. F. Zhang, A. A. Sousa, A. Masedunskas, R. D. Leapman, R. Weigert, J. S. Gutkind, J. F. Rusling, *Acs Nano* **2009**, *3*, 307–316.

[6] Q. W. Fan, W. A. Weiss, *Oncogene* **2005**, *24*, 829–837.

[7] E. Arwert, S. Hingtgen, J. L. Figueiredo, H. Bergquist, U. Mahmood, R. Weissleder, K. Shah, *Cancer Res.* **2007**, *67*, 7335–7342.

[8] a) A. Veeravagu, Z. F. Liu, G. Niu, K. Chen, B. Jia, W. B. Cai, C. J. Jin, A. R. Hsu, A. J. Connolly, V. Tse, F. Wang, X. Y. Chen, *Clin. Cancer Res.* **2008**, *14*, 7330–7339; b) M. S. Lesniak, H. Brem, *Nat. Rev. Drug Discovery* **2004**, *3*, 499–508.

[9] a) A. J. Ekstrand, N. Sugawa, C. D. James, V. P. Collins, *Proc. Natl. Acad. Sci. USA* **1992**, *89*, 4309–4313; b) P. A. Humphrey, A. J. Wong, B. Vogelstein, M. R. Zalutsky, G. N. Fuller, G. E. Archer, H. S. Friedman, M. M. Kwatra, S. H. Bigner, D. D. Bigner, *Proc. Natl. Acad. Sci. USA* **1990**, *87*, 4207–4211.

[10] a) I. Vivanco, C. L. Sawyers, *Nat. Rev. Cancer* **2002**, *2*, 489–501; b) F. Yamoutpour, V. Bodernpudi, S. E. Park, W. H. Pan, M. J. Mauzy, R. A. Kratzke, A. Dudek, D. A. Potter, R. A. Woo, D. M. O'Rourke, D. J. Tindall, F. Farassati, *Mol. Cancer Ther.* **2008**, *7*, 3586–3597.

[11] a) J. J. Li, Y. A. Wang, W. Z. Guo, J. C. Keay, T. D. Mishima, M. B. Johnson, X. G. Peng, *J. Am. Chem. Soc.* **2003**, *125*, 12567–12575; b) R. G. Xie, U. Kolb, J. X. Li, T. Basche, A. Mews, *J. Am. Chem. Soc.* **2005**, *127*, 7480–7488.

[12] a) W. Liu, M. Howarth, A. B. Greytak, Y. Zheng, D. G. Nocera, A. Y. Ting, M. G. Bawendi, *J. Am. Chem. Soc.* **2008**, *130*, 1274–1284; b) K. Susumu, H. T. Uyeda, I. L. Medintz, T. Pons, J. B. Delehanty, H. Mattoussi, *J. Am. Chem. Soc.* **2007**, *129*, 13987–13996.

[13] a) S. Kida, M. Maeda, K. Hojo, Y. Eto, S. Nakagawa, K. Kawasaki, *Chem. Pharm. Bull.* **2007**, *55*, 685–687; b) A. S. M.

Kamruzzahan, A. Ebner, L. Wildling, F. Kienberger, C. K. Riener, C. D. Hahn, P. D. Pollheimer, P. Winklehner, M. Holzl, B. Lackner, D. M. Schorkl, P. Hinterdorfer, H. J. Gruber, *Bioconjugate Chem.* **2006**, *17*, 1473–1481; c) S. Bauhuber, C. Hozsa, M. Breunig, A. Göpferich, *Adv. Mater.* **2009**, *21*, 3286–3306.

[14] Y. L. Chiu, A. Ali, C. Y. Chu, H. Cao, T. M. Rana, *Chem. Biol.* **2004**, *11*, 1165–1175.

[15] J. Xie, K. Chen, H. Y. Lee, C. J. Xu, A. R. Hsu, S. Peng, X. Y. Chen, S. H. Sun, *J. Am. Chem. Soc.* **2008**, *130*, 7542.

[16] W. B. Cai, D. W. Shin, K. Chen, O. Gheysens, Q. Z. Cao, S. X. Wang, S. S. Gambhir, X. Y. Chen, *Nano Lett.* **2006**, *6*, 669–676.

[17] a) C. C. Berry, *Nanomedicine* **2008**, *3*, 357–365; b) G. Ruan, A. Agrawal, A. I. Marcus, S. Nie, *J. Am. Chem. Soc.* **2007**, *129*, 14759–14766.

[18] a) A. M. Derfus, W. C. W. Chan, S. N. Bhatia, *Nano Lett.* **2004**, *4*, 11–18; b) C. Kirchner, T. Liedl, S. Kudera, T. Pellegrino, A. M. Javier, H. E. Gaub, S. Stolzle, N. Fertig, W. J. Parak, *Nano Lett.* **2005**, *5*, 331–338.

[19] a) A. Meyer, C. M. van Golen, B. Kim, K. L. van Golen, E. L. Feldman, *Neoplasia* **2004**, *6*, 332–342; b) L. Martiniova, E. W. Lai, A. G. Elkahloun, M. Abu-Asab, A. Wickremasinghe, D. C. Solis, S. M. Perera, T. T. Huynh, I. A. Lubensky, A. S. Tischler, R. Kvetnansky, S. Alesci, J. C. Morris, K. Pacak, *Clin. Exp. Metastasis* **2009**, *26*, 239–250; c) Z. B. Li, W. B. Cai, Q. Z. Cao, K. Chen, Z. H. Wu, L. N. He, X. Y. Chen, *J. Nucl. Med.* **2007**, *48*, 1162–1171.

[20] M. Y. Wang, K. V. Lu, S. J. Zhu, E. Q. Dia, I. Vivanco, G. M. Shackleford, W. K. Cavenee, I. K. Mellinghoff, T. F. Cloughesy, C. L. Sawyers, P. S. Mischel, *Cancer Res.* **2006**, *66*, 7864–7869.